ELSEVIER

Journal of Molecular Structure 516 (2000) 99–106

Journal of
MOLECULAR
STRUCTURE

www.elsevier.nl/locate/molstruc

Luminescence studies of dinuclear gold(I) phosphor-1,1-dithiolate complexes

W.E. van Zyl[a], J.M. López-de-Luzuriaga[b], J.P. Fackler Jr.[a]*

[a]*Department of Chemistry and Laboratory for Molecular Structure and Bonding, Texas A&M University, P.O. Box 30012, College Station, TX 77842-3012, USA*

[b]*Departamento de Química, Universidad de La Rioja, Obispo Bustamante 3, E-26001 Logroño, Spain*

Received 20 April 1999; accepted 23 April 1999

Abstract

Luminescence properties of several structurally characterized dinuclear gold(I) complexes with phosphor-1,1-dithiolato type ligands were investigated. Among these complexes, single crystal X-ray analyses revealed structural types, where weak intermolecular Au···Au interactions (~2.90–3.20 Å) were present in some cases and absent in others. This interaction showed a profound influence on the observed emission spectra for the title complexes. A clear correlation between the emission profiles of these gold–sulfur complexes and the presence of intermolecular Au···Au interactions in the solid state has been established.

Keywords: Dinuclear gold–sulfur complexes; Luminescence properties; Phosphor-1,1-dithiolates

1. Introduction

Presence of weak intermolecular metal–metal interactions has been implicated in the design of electronic and sensor devices [1–4]. Gold–sulfur complexes often show weak intermolecular bonding interactions (5–15 kcal mol^{-1}) between the closed shell d^{10} gold atoms. This phenomenon is termed 'aurophilicity', with an origin best described by relativistic and correlation effects [5–7]. Energies associated with crystal packing effects often dominate the aurophilicity, however, and thus dictate whether weak interactions will be present or absent in the crystalline solid. For this reason, attempts to determine the presence of such interactions by means other than X-ray crystallographic study have been frustrated. The problem is further compounded where growth of single crystals is not readily achieved where, for example, the products are amorphous solids such as the anti-arthritic gold–sulfur drugs Myochrysine and Solganol [8]. Indeed, although the crystal structure of Myochrysine have recently been reported, suitable crystals could only be obtained in an unconventional manner after numerous other strategies failed [9]. The solid state structure of Solganol is still uncertain.

A method that could qualitatively detect the presence of intermolecular Au···Au interactions in the bulk solid sample would have clear benefits, one of which may provide information about the biological function of the aforementioned gold–sulfur drugs. Investigations to find a relationship between the observation of emission and the presence of weak intermolecular bonding interactions between neighboring gold atoms have been addressed

* Corresponding author. Tel.: + 1-409-845-0648; fax: + 1-409-845-3154.

E-mail address: fackler@mail.chem.tamu.edu (J.P. Fackler Jr.)

0022-2860/00/$ - see front matter
PII: S0022-2860(99)00231-8

previously [10–12], but a conclusive answer has not been obtained. Here we report the luminescence properties of several closely related dinuclear gold–sulfur complexes and show how their emission profile relates to the solid state structure in each case. In particular, the presence or absence of Au···Au interactions was found to be accurately predicted for all complexes investigated, based solely on the complex's emission profile. The synthesis and single crystal X-ray structure of $[AuS_2PPh(OCH_2CH{=}CH_2)]_2$ **1** is included in the present study as a representative example of the title compounds. Since this study is aimed at the luminescence properties of the title complexes, a detailed account of the synthesis, structure and reactivity of these complexes will be published elsewhere.

2. Experimental

2.1. General

The ^{1}H NMR spectrum of **1** was obtained on a Varian XL-200 spectrometer operating at 200 MHz, and is expressed in parts per million (ppm) downfield shift referenced internally to the residual proton impurity in the deuterated solvent, and is reported as: chemical shift position (δ_H); multiplicity (s = singlet, d = doublet, m = multiplet, br = broad); relative integral; and assignment. The $^{31}P\{^1H\}$ NMR spectrum of **1** was obtained on a Varian XL 200 MHz broadband spectrometer operating at 81 MHz, with chemical shifts reported relative to a 85% H_3PO_4 in D_2O external standard solution. The positive fast atom bombardment (+FAB/DIP (direct insertion probe)) mass spectrum was acquired on a VG Analytical (Manchester, UK) 70S high resolution, double focusing mass spectrometer.

2.2. Preparation of $[AuS_2PPh(OCH_2CH{=}CH_2)]_2$ **1**

A 50 ml Schlenk tube was charged with $[NH_4][S_2PPh(OCH_2CH{=}CH_2)]$ (79 mg, 0.32 mmol) and placed under vacuum for 30 min. The salt was dissolved in 20 ml THF, and upon dissolution ClAuTHT (100 mg, 0.31 mmol) was added in one portion at room temperature. An immediate white precipitate (NH_4Cl) was observed. The mixture was stirred for 40 min followed by removal of the solvent in vacuo. The complex was extracted with CH_2Cl_2 (25 ml) and filtered through anhydrous $MgSO_4$ to remove NH_4Cl. The filtrate was evaporated under reduced pressure, which afforded a pale yellow powder. The crude material was washed with three 10 ml portions of ether, and dried under vacuum (10^{-2} Torr) for 1 h; mp: 144°C. +FAB/DIP MS (NBA/$CHCl_3$, *m/z*): 853 ($[M+1]^+$), 655 ($[M\text{-}Au]^+$), 427 ($[M\text{-}AuL]^+$). ^{1}H NMR data for *cis* and *trans* isomers (chloroform-d_1, 300 MHz, 20°C, δ): 8.11–8.01 (m, 4H, Ph), 7.61–7.44 (m, 6H, Ph), 6.10–5.90 (m-br, 2H, C*H*=CH_2), 5.46 (d, 4H, OCH_2), 5.30 (d, 4H, OCH_2), 4.88 (s-br, 4H, C=CH_2). $^{31}P\{^1H\}$ NMR data for *cis* and *trans* isomers (chloroform-d_1, 200 MHz, 19°C, δ): 106.18 (s), 103.37(s).

2.3. Luminescence studies

Excitation and emission spectra were obtained on a SLM/AMINCO, Model 8100 spectrofluorometer

Table 1
Crystal data and structure refinement for $[AuS_2PPh(OCH_2CH{=}CH_2)]_2$ **1**

Empirical formula	$C_{18}H_{20}Au_2O_2P_2S_4$
Formula weight	852.45
Temperature	293(2) K
Wavelength	0.71073 Å
Crystal system	Triclinic
Space group	$P\bar{1}$
Unit cell dimensions	$a = 9.559(2)$ Å, $\alpha = 103.21(3)°$ $b = 12.283(3)$ Å, $\beta = 110.42(3)°$ $c = 12.547(3)$ Å, $\gamma = 105.16(3)°$
Volume, *Z*	1246.5(4) Å^3, 2
Density (calculated)	2.271 mg m^{-3}
Absorption coefficient	12.231 mm^{-1}
F(000)	792
Crystal size	0.08 × 0.08 × 0.28 mm^3
θ range for data collection	2.10–22.49°
Limiting indices	$-10 \le h \le 9$, $-13 \le k \le 12$, $0 \le l \le 13$
Reflections collected	3258
Independent reflections	3258 [*R*(int) = 0.0000]
Refinement method	Full-matrix least-squares on F^2
Data/restraints/parameters	3258/62/254
Goodness-of-fit on F^2	1.038
Final *R* indices [$I > 2\sigma(I)$]	$R1 = 0.0408$, $wR2 = 0.0896$
R indices (all data)	$R1 = 0.0575$, $wR2 = 0.0955$
Extinction coefficient	0.0329(9)
Largest difference peak and hole	0.776 and −0.971 e Å^{-3}

Table 2
Selected bond lengths (Å) and angles (°) for $[AuS_2PPh(OCH_2CH{=}CH_2)]_2$ **1** (symmetry transformations used to generate equivalent atoms: #1: $-x+1, -y+1, -z+1$; #2: $-x+1, -y, -z+1$)

Au(1)–S(1)	2.299(3)
Au(1)–S(2)#1	2.310(3)
Au(1)–Au(2)	3.0963(9)
Au(1)–Au(1)#1	3.1231(11)
P(1)–O(1)	1.576(10)
P(1)–C(11)	1.792(12)
P(1)–S(2)	2.006(5)
P(1)–S(1)	2.008(4)
S(2)–Au(1)#1	2.310(3)
Au(2)–S(4)#2	2.290(4)
Au(2)–S(3)	2.301(4)
Au(2)–Au(2)#2	3.1171(10)
P(2)–O(2)	1.588(14)
P(2)–C(21)	1.73(2)
P(2)–S(3)	1.993(5)
P(2)–S(4)	2.013(5)
S(4)–Au(2)#2	2.290(4)
C(11)–C(12)	1.376(12)
C(11)–C(16)	1.382(12)
C(12)–C(13)	1.380(12)
C(13)–C(14)	1.366(13)
C(14)–C(15)	1.366(13)
C(15)–C(16)	1.383(12)
C(21)–C(26)	1.296(13)
C(21)–C(22)	1.323(14)
C(22)–C(23)	1.333(14)
C(23)–C(24)	1.31(2)
C(24)–C(25)	1.31(2)
C(25)–C(26)	1.329(14)
O(1)–C(1)	1.427(12)
C(1)–C(2)	1.45(2)
C(2)–C(3)	1.35(2)
O(2)–C(4)	1.36(3)
C(4)–C(5)	1.44(3)
C(5)–C(6)	1.40(3)
S(1)–Au(1)–S(2)#1	172.38(11)
S(1)–Au(1)–Au(2)	84.68(8)
S(2)#1–Au(1)–Au(2)	88.26(S(1)
S(1)–Au(1)–Au(1)#1	93.33(8)
S(2)#1–Au(1)–Au(1)#1	94.29(8)
Au(2)–Au(1)–Au(1)#1	160.33(3)
O(1)–P(1)–C(11)	107.1(5)
O(1)–P(1)–S(2)	114.4(4)
C(11)–P(1)–S(2)	107.7(4)
O(1)–P(1)–S(1)	104.8(4)
C(11)–P(1)–S(1)	104.7(4)
S(2)–P(1)–S(1)	117.4(2)
P(1)–S(1)–Au(1)	102.9(2)
P(1)–S(2)–Au(1)#1	101.6(2)
S(4)#2–Au(2)–S(3)	172.31(11)
S(4)#2–Au(2)–Au(1)	90.17(9)
S(3)–Au(2)–Au(1)	82.55(9)
S(4)#2–Au(2)–Au(2)#2	92.10(9)
S(3)–Au(2)–Au(2)#2	95.47(9)
Au(1)–Au(2)–Au(2)#2	170.84(3)
O(2)–P(2)–C(21)	102.3(8)
O(2)–P(2)–S(3)	112.6(6)
C(21)–P(2)–S(3)	106.6(5)
O(2)–P(2)–S(4)	110.4(6)
C(21)–P(2)–S(4)	106.3(5)
S(3)–P(2)–S(4)	117.3(2)
P(2)–S(3)–Au(2)	101.7(2)
P(2)–S(4)–Au(2)#2	104.1(2)
C(12)–C(11)–C(16)	116.8(13)
C(12)–C(11)–P(1)	122.1(10)
C(16)–C(11)–P(1)	121.1(9)
C(11)–C(12)–C(13)	121.3(14)
C(14)–C(13)–C(12)	121(2)
C(15)–C(14)–C(13)	117(2)
C(14)–C(15)–C(16)	122(2)
C(11)–C(16)–C(15)	121.2(14)
C(26)–C(21)–C(22)	108(2)
C(26)–C(21)–P(2)	128(2)
C(22)–C(21)–P(2)	123.7(13)
C(21)–C(22)–C(23)	127(2)
C(24)–C(23)–C(22)	125(2)
C(25)–C(24)–C(23)	108(2)
C(24)–C(25)–C(26)	128(2)
C(21)–C(26)–C(25)	125(2)
C(1)–O(1)–P(1)	126.6(10)
O(1)–C(1)–C(2)	116(2)
C(3)–C(2)–C(1)	99(2)
C(4)–O(2)–P(2)	132(2)
O(2)–C(4)–C(5)	123(3)
C(6)–C(5)–C(4)	94(3)

using a xenon lamp. The radiation was filtered through a 0.10 M KNO_2 solution to reduce the amount of scattered light. Low-temperature measurements were made in a cryogenic device of local design. Collodion was used to attach the powder samples to the holder. The collodion was scanned for a baseline subtraction. Liquid nitrogen was used to obtain the 77 K measurements.

2.4. Crystallography

A single crystal of **1** suitable for X-ray crystallographic studies was obtained as a pale yellow needle from a CH_2Cl_2 solution layered with hexane. The crystal was mounted on the tip of a quartz fiber with fast-adhesive glue. Single crystal diffraction analysis

Table 3
Atomic coordinates ($\times 10^4$) and equivalent isotropic displacement parameters ($Å^2 \times 10^3$) for the complex $[AuS_2PPh(OCH_2CH{=}CH_2)]_2$ **1**. *U*(eq) is defined as one-third of the trace of the orthogonalized U_{ij} tensor

Atom	*x*	*y*	*z*	*U*(eq)
Au(1)	5384(1)	3913(1)	5292(1)	62(1)
P(1)	7014(4)	5132(3)	3646(3)	63(1)
S(1)	6246(5)	3516(3)	3802(3)	79(1)
S(2)	5392(5)	5895(3)	3147(3)	83(1)
Au(2)	4981(1)	1289(1)	5140(1)	65(1)
P(2)	7240(4)	923(3)	7640(3)	72(1)
S(3)	7238(5)	2246(3)	6971(3)	91(1)
S(4)	7313(5)	−578(3)	6639(3)	89(1)
C(11)	7713(14)	4874(10)	2494(10)	67(3)
C(12)	6741(21)	4620(16)	1291(11)	116(6)
C(13)	7229(23)	4282(18)	396(15)	136(7)
C(14)	8759(21)	4316(15)	676(15)	120(6)
C(15)	9747(20)	4596(14)	1871(14)	110(5)
C(16)	9246(16)	4877(13)	2771(14)	95(4)
C(21)	8955(20)	1507(13)	9003(12)	97(5)
C(22)	10371(20)	2230(22)	9172(19)	176(9)
C(23)	11730(27)	2709(27)	10196(20)	236(13)
C(24)	11892(27)	2489(21)	11197(20)	185(11)
C(25)	10520(25)	1686(23)	10974(19)	210(11)
C(26)	9149(25)	1225(17)	9965(13)	156(8)
O(1)	8539(11)	5932(8)	4887(8)	93(3)
C(1)	9177(21)	7216(12)	5423(15)	120(6)
C(2)	10512(34)	7856(29)	5218(38)	336(32)
C(3)	9760(33)	8378(27)	4482(24)	269(20)
O(2)	5846(19)	583(14)	8058(12)	148(5)
C(4)	4436(41)	772(45)	7773(40)	377(32)
C(5)	3497(65)	620(46)	8450(58)	430(36)
C(6)	3405(78)	−562(32)	8329(30)	659(75)

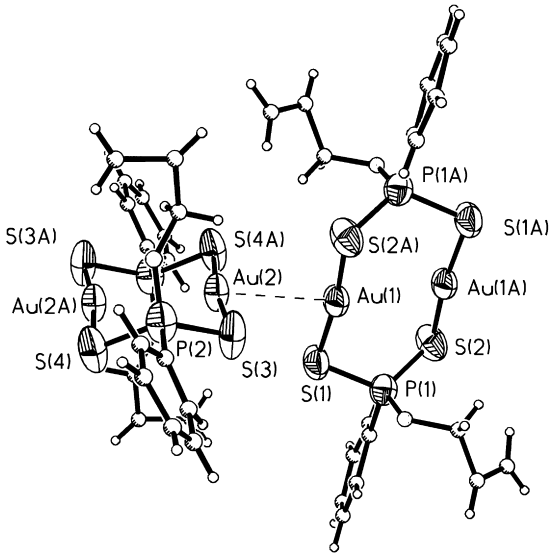

Fig. 1. A perspective view of the molecular structure of **1** showing the atom labeling scheme. Only the atoms in the metallocycle are shown as thermal ellipsoids at the 50% probability level. All other atoms are of arbitrary size.

was carried out on an automated Nicolet R3 four-circle diffractometer utilizing the Wyckoff scanning technique with graphite monochromated Mo-K_α ($\lambda = 0.71073$ Å) radiation. Refined cell parameters were determined from setting angles of 25 reflections with $20 < 2\theta < 30°$. The unit cell was determined using the search, center, index, and least squares refinement routine. The Laue class and lattice dimensions were verified by axial oscillation photography. The intensity data were corrected for absorption, Lorentz and polarization effects. An empirical absorption correction was performed based on ψ scans of five strong reflections spanning a range of 2θ values. All data processing were performed on a Data General Eclipse S140 minicomputer using the SHELXTL crystallographic package (version 5.1) and Siemens SHELXTL PLUS (Micro Vax II) [13]. The systematic absences were consistent with the assigned space group. The crystal structure was solved using direct methods to determine the gold atom position, while all other atoms were located with difference Fourier maps. Structure refinement was carried out using SHELX-93. The position of the hydrogen atoms were calculated by assuming idealized geometries, C–H = 0.93 Å. The relevant crystal data and structure refinement for **1** are shown in Table 1. The selected bond lengths (Å) and angles (°) for **1** are shown in Table 2. Atomic coordinates ($\times 10^4$) and equivalent isotropic displacement parameters ($Å^2 \times 10^3$) for **1** are shown in Table 3.

3. Results and discussion

The luminescence properties of a number of structurally characterized gold–sulfur complexes were investigated. Some of these compounds show intermolecular Au···Au bonding. All the complexes in this study luminesce at 77 K in the solid state. The complex $[AuS_2PPh(OCH_2CH{=}CH_2)]_2$ **1** contains intermolecular Au···Au interactions, and its

Table 4
Solid state luminescence data for dinuclear gold(I)–sulfur compounds

Complex	298 (K)		77 (K)	
	Excitation (nm)	Emission (nm)	Excitation (nm)	Emission (nm)
$[AuS_2PPh(OC_3H_5)]_2$[a] **1**	400	443	400	445, 491
$[AuS_2PPh_2]_2$[a]	400	461	380	451, 495
$[AuS_2PPh(OEt)]_2$[a]	398	447	400	453, 496
$[AuS_2P(4\text{-}C_6H_4OMe)(OEt)]_2$[b]	392	467	395	453, 494
$[AuS_2PPh(OC_5H_9)]_2$[c]	398	487	396	491, 530
$[AuS_2P(O^iPr)_2]_2$[c]	400	440	400	435, 610
$[AuS_2P(4\text{-}C_6H_4OMe)(OSiPh_3)]_2$[c] **2**			319	417
$[AuS_2P(4\text{-}C_6H_4OMe)(O\text{-menthyl})]_2$[c]			320	447
$[AuS_2PEt_2]$[c]			338	423
$[AuS_2PMe_2]_2$[c]			327	421
$[NBu_4]_2[Au_2\{S_2C{=}C(CN)_2\}]$[c]			388	495, 527
$K_2[S_2C{=}C(CN)_2]$			468 (fine)	553

[a] Complexes with intermolecular Au···Au (~ 3.1 Å) interactions.
[b] Structure not determined.
[c] Complexes with no intermolecular Au···Au interactions.

molecular structure is shown in Fig. 1. The structure is a neutral eight membered metallocycle in an elongated chair conformation with short transannular gold–gold (~3.1 Å) interactions. The selected bond lengths (Å) and angles (°) for **1** are shown in Table 2. The luminescence spectrum of **1** is shown in Fig. 2. The complex $[AuS_2P(4\text{-}C_6H_4OCH_3)(OSiPh_3)]_2$ **2** is a representative example of a complex with no intermolecular interactions. It was previously reported by two of us [14]. The luminescence spectra of **2** is shown in Fig. 3. All other compounds examined (see Table 4) show a similar excitation and emission profile as obtained for **1** and **2**. The observation that the emission wavelength is different for **1** and **2** suggests that the excitation is from the sulfur orbital of the ligand, and not from a π orbital associated with

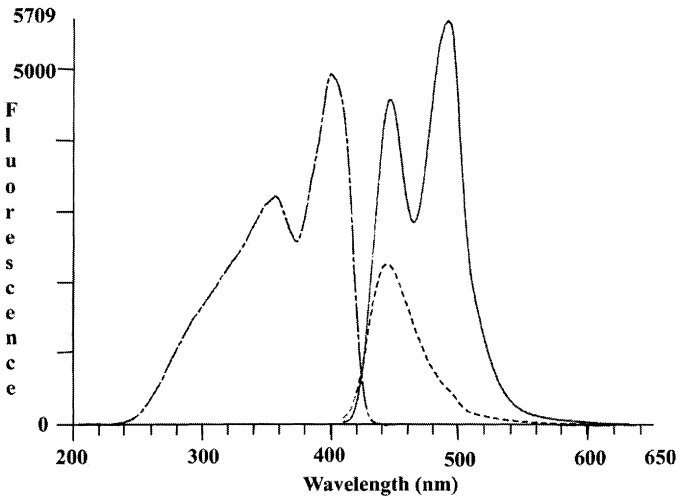

Fig. 2. Excitation (— - —) at room temperature, emission at room temperature (- - -), and emission at 77 K (—) spectra for **1**.

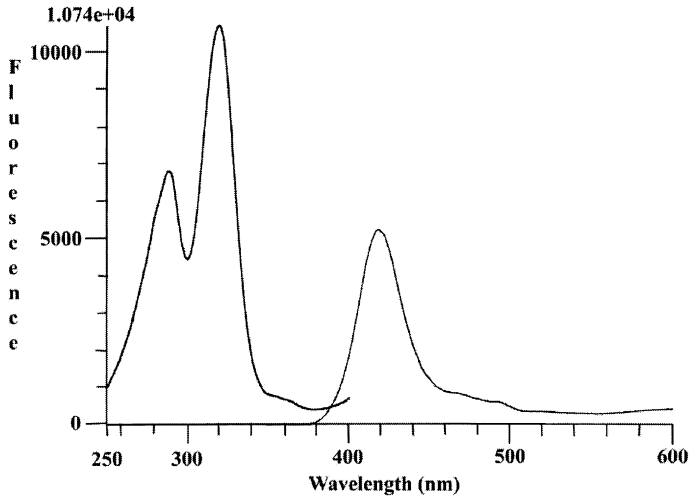

Fig. 3. Excitation and emission spectra of **2** at 77 K.

a phenyl group, since a large change in energy difference would not be anticipated in the latter case. Thus, these emissions can be assigned as ligand-to-metal charge-transfer (LMCT), similar to other dinuclear gold(I) complexes bonded to sulfur, with the excitation associated with a sulfur-to-metal based orbital in the excited state.

The blue shift observed in the emission bands with increasing temperature is consistent with an increase in Au–Au separation as a result of thermal expansion. This fact seems to indicate that the Au–Au distance has a significant influence on the HOMO–LUMO gap, which increases with increasing Au–Au separation distance. Correlations of emission energies with the Au–Au distance do exist [15] showing that the emission energy is sensitive to this variable. In the series of dithiophosphonates reported here, the donor properties of the different substituents on the phosphorus centers are virtually the same, and are not considered responsible for the shifts.

When a spectral measurement for **1** is carried out in dilute $CHCl_3$ solutions ($\sim 10^{-4}$ M), the yellow color disappears and the emission is quenched, but it keeps the color and optical properties in concentrated solutions (> 0.1 M) where the molecules must be closely associated. The absorption spectra of **1** measured at 0.1, 0.03 and 0.01 M concentrations show a progressive blue shift of the charge transfer absorption, and the disappearance of a very low intensity broad band placed at ~400 nm which is assigned to the transition observed in emission. Concentration dependent UV–vis spectra in gold(I) compounds were reported as an evidence of molecular association [16], but to our knowledge no study have previously shown a clear correlation between emission and structure at a variable temperature in the solid state. All of these facts seem to indicate that although the emission is assigned to a LMCT transition, the Au···Au interactions have a systematic influence on the energies of the frontier orbitals responsible for the emission. In fact, as previously reported [10], the effect of Au···Au interactions produce a destabilization of the d_{z^2} orbital (where the *z*-axis is along the direction of the metal–metal interaction), while the empty $6p_z$ orbital is stabilized. This would have the net effect of lowering the energy of the transition producing a red shift of the emission energy. As the number of Au···Au interactions increases, the HOMO–LUMO gap is reduced.

The high energy band in **1** appears to result from fluorescence (due to the small Stokes shift) and lower energy band from phosphorescence. The latter band presumably is related to the close proximity of the gold centers, because it disappears when there are no interaction between two adjacent molecules. In order to determine if there is a general trend emanating from these luminescence studies, we investigated the previously reported complexes

$[AuS_2P(O^iPr)_2]_2$, which shows intra- and intermolecular Au···Au interactions [17], and $[AuS_2PMe_2]_2$ which shows only intramolecular Au···Au interactions [18]. The luminescence properties of all these complexes are consistent with results obtained in the present study. In the former complex, the room temperature emission spectrum shows one band, while at 77 K, it shows two (see Table 4). The latter complex is non-emissive at room temperature and shows one emission band at 77 K at 421 nm and at a maximum excitation energy of 327 nm.

This study revealed that the presence or absence of intermolecular Au···Au interactions in the solid state have a profound influence on the nature of the luminescence the compounds exhibit. Specifically, a lower energy emission had been observed only at a low temperature (77 K), which became faint and "disappeared" as the temperature was increased. The first possible explanation to account for the origin of this unusual fact is that the excited state that gives rise to the emission only connects with the higher energy state as the temperature increases (thus populating higher vibrational levels). As the temperature is lowered, the molecules remain in the excited energy level for a longer period, eventually crossing over into a different state which gives rise to a second emission band. A second possible explanation considered is a second-order phase transition in the structure, which traps the low energy excited state. Subsequent experiments have ruled this out, however, based on X-ray crystallographic studies performed on a single crystal of the complex $[AuS_2PPh_2]_2$. Data were collected at 213 and 293 K and the structure solved, but the results indicated only a small change (0.02 Å) in the Au···Au interactions, not significant enough to consider a second-order phase transition.

Recently, Eisenberg and co-workers reported [1] two forms of a dinuclear gold(I) dithiocarbamate complex. The one form contains intermolecular interactions (solvated) and the other form contains no intermolecular interactions (not solvated). The luminescence properties of both forms are in accordance with our results. The former shows one emission (630 nm) band and the latter shows no emission, both at room temperature. We expect different results at 77 K for both forms; i.e. the form with the one emission band at room temperature should reveal two bands, and the non-luminescent form will reveal one band. The ability to predict the presence of weak intermolecular Au···Au interactions with a different gold–sulfur system was tested for the complex $[NBu_4]_2[Au_2\{S_2C{=}C(CN)\}_2]$, of which the structure is known [19] and shows no intermolecular Au···Au interactions. The complex is also dinuclear, but has a S–C–S bridging moiety as opposed to the S–P–S moiety presented throughout this paper. Interestingly, the complex showed two emission bands (495, 527 nm) at 77 K, which apparently contradict the theory presented in the present study. Subsequent studies proved, however, that the yellow potassium salt as a free ligand luminesce at 77 K with an emission at 553 nm. The 527 nm emission of the complex was thus attributed to the ligand since it had the same emission profile. This phenomenon was not seen for any of the other complexes investigated which all had colorless free ligands.

In conclusion, study of the series of complexes reported here suggests that the emission profile alone is a useful predictor of the presence of intermolecular linear chain Au···Au interactions for the dinuclear gold(I)–sulfur compounds. We expect the results to be extended to other dinuclear gold–sulfur systems and possibly even other gold(I)–sulfur compounds wherein Au···Au interactions influence the LUMO and hence the emission spectra.

Acknowledgements

The authors acknowledge the Robert A. Welch Foundation. J.M.L-de-L. acknowledges the financial support from the University of La Rioja. We thank Mr R. Theron Stubbs for assistance with the structure refinement of **1**.

References

[1] M.A. Mansour, W.B. Connick, R.J. Lachicotte, H.J. Gysling, R. Eisenberg, J. Am. Chem. Soc. 120 (1998) 1329.
[2] J.S. Miller, A.J. Epstein, Prog. Inorg. Chem. 20 (1976) 1.
[3] C.A. Daws, C.L. Exstrom, J.R. Sowa, K.R. Mann, Chem. Mater. 9 (1997) 363.
[4] Y. Konugi, K.R. Mann, L.L. Miller, C.L. Exstrom, J. Am. Chem. Soc. 120 (1998) 589.
[5] J. Li, P. Pyykkö, Chem. Phys. Lett. 197 (1992) 586.
[6] P. Pyykkö, L. Li, N. Runeberg, Chem. Phys. Lett. 218 (1994) 133.

[7] P. Pyykkö, Chem. Rev. 3 (1997) 597.
[8] R.C. Elder, K. Ludwig, J.N. Cooper, M.K. Eidsness, J. Am. Chem. Soc. 107 (1985) 5024.
[9] R. Bau, J. Am. Chem. Soc. 120 (1998) 9380.
[10] J.M. Forward, D. Bohmann, J.P. Fackler Jr, R.J. Staples, Inorg. Chem. 34 (1995) 6330.
[11] R. Narayanaswamy, M.A. Young, E. Parkhurst, M. Ouellette, M.E. Kerr, D.M. Ho, R.C. Elder, A.E. Bruce, M.R.M. Bruce, Inorg. Chem. 32 (1993) 2506.
[12] W.B. Jones, J. Yuan, R. Narayanaswamy, M. Young, R.C. Elder, A.E. Bruce, M.R.M. Bruce, Inorg. Chem. 34 (1995) 1996.
[13] G.M. Sheldrick, SHELXTL-PLUS User's Manual, Nicolet, XRD Corp., Madison, WI, 1988.
[14] W.E. van Zyl, R.J. Staples, J.P. Fackler, Inorg. Chem. Commun. 1 (1998) 51.
[15] Z. Assefa, B.G. McBurnett, R.J. Staples, J.P. Fackler Jr., B. Assmann, K. Angermaier, H. Schmidbaur, Inorg. Chem. 33 (1995) 75–83 Erratum: Inorg. Chem. (1995) 2490.
[16] F.-D. Feng, S.S. Tang, C.W. Liu, I.J.B. Lin, Y.-S. Wen, L.-K. Liu, Organometallics 16 (1997) 909.
[17] S.L. Lawton, W.J. Rohrbaugh, G.T. Kokotailo, Inorg. Chem. 11 (1972) 2227.
[18] M. Preisenberger, A. Bauer, A. Schier, H. Schmidbaur, J. Chem. Soc., Dalton Trans. (1997) 4753.
[19] M.N.I. Khan, S. Wang, J.P. Fackler Jr, Inorg. Chem. 28 (1989) 3579.